Solid lipid nanoparticles of ondansetron HCl for intranasal delivery: development, optimization and evaluation

Ashwini S. Joshi · Hitesh S. Patel · Veena S. Belgamwar ·
Anshuman Agrawal · Avinash R. Tekade

Abstract The present investigation deals with the development and statistical optimization of solid lipid nanoparticles (SLNs) of ondansetron HCl (OND) for intranasal (i.n.) delivery. SLNs were prepared using the solvent diffusion technique and a 2^3 factorial design. The concentrations of lipid, surfactant and cosurfactant were independent variables in this design, whereas, particle size and entrapment efficiency (EE) were dependent variables. The particle size of the SLNs was found to be 320–498 nm, and the EE was between 32.89 and 56.56 %. The influence of the lipid, surfactant and cosurfactant on the particle size and EE was studied. A histological study revealed no adverse response of SLNs on sheep nasal mucosa. Transmission electron microscopic analysis showed spherical shape particles. Differential scanning calorimetry and X-ray diffraction studies indicated that the drug was completely encapsulated in a lipid matrix. In vitro drug release studies carried out in phosphate buffer (pH 6.6) indicated that the drug transport was of Fickian type. Gamma scintigraphic imaging in rabbits after i.n. administration showed rapid localization of the drug in the brain. Hence, OND SLNs is a promising nasal delivery system for rapid and direct nose-to-brain delivery.

A. S. Joshi · H. S. Patel · V. S. Belgamwar
Department of Pharmaceutics, R.C. Patel Institute
of Pharmaceutical Education and Research, Shirpur, India

A. Agrawal
Department of Nuclear Medicine, Shri. Siddhivinayak Ganapati
Cancer Hospital, Sangli Road, Miraj, India

A. R. Tekade (✉)
Department of Pharmaceutics, Rajarshi Shahu College
of Pharmacy and Research, Mumabi-Pune Bypass Highway,
Tathawade, Pune 411033, India
e-mail: avitekade@gmail.com

1 Introduction

Development of drug delivery carriers is often very challenging due to the physico-chemical properties of the drugs involved. Poor solubility, a low permeability, short half-life, and a high molecular weight are the common challenges faced by those involved in formulating drug delivery systems. The importance of carriers is well known and therefore various colloidal drug carrier systems have been developed, including liposomes, dendrimers, solid lipid nanoparticles (SLN) and polymeric nanoparticles. SLNs, as the most novel carriers, have attracted the greatest attention among these. The main reasons for the interest in these carriers are their components, the size and narrow size distribution, their biocompatibility, and the different possible administration routes [1]. Further, SLNs offer other advantages such as drug targeting, controlled drug release, better drug stability, the possibility of incorporation of lipophilic and hydrophilic drugs, ease of scaling up, the possibility of sterilization, and good tolerability. However, SLNs also have a few drawbacks such as low drug loading and unpredictable drug release [2–5].

SLNs are commonly produced using techniques based on high pressure homogenization, microemulsion and solvent emulsification/evaporation. The solvent diffusion method is another technique used to prepare SLNs. It is commonly used for preparation of liposomes and polymeric nanoparticles. It offers clear advantages over other existing methods such as the ease of handling, and faster production process without any sophisticated equipments. In this technique, drugs and lipids are dissolved in a water-miscible organic solvent (chloroform, ethanol, acetone, etc.) at an elevated temperature and injected into an aqueous surfactant solution with continuous mechanical stirring [6]. The process depends on the water-miscibility

of the solvents. When the organic phase is injected into water, the drug dissolved in the organic solvent solidifies instantly due to diffusion of the organic solvent from the droplets into the continuous phase [7].

In recent years, the nasal route has received much attention being a convenient and reliable route for systemic administration of drugs. It is considered a promising alternative administration route wherein drugs may be targeted directly to the brain via olfactory neurons, allowing a drug to enter the central nervous system (CNS) more effectively. Drugs administered by the intranasal (i.n.) route not only circumvent the blood–brain barrier (BBB) but also are not subjected to the hepatic first pass effect. Moreover, the nasal route is non-invasive. Along with a reduced risk of infection, it offers the convenience and ease of self-medication and a resulting improved patient compliance. One of the most important parameters to be considered here is nasal mucociliary clearance, which limits the duration of drug absorption. Till date little has been reported on nasal delivery of SLNs possibly because of limited success due to difficulties such as mucoadhesion and mucociliary clearance.

In this study, ondansetron HCl (OND) SLNs were formulated and evaluated for nasal delivery. OND is a serotonin (5-hydroxy tryptamine) subtype (5HT3) receptor antagonist used in the management of chemotherapy induced postoperative nausea and vomiting. Its absolute bioavailability is about 60 % due to its first pass metabolism. It has a log P value of 2.4 and plasma half life of about 3–4 h [8].

Optimization using factorial designs is a powerful, efficient and systematic means of shortening the time required for development of pharmaceutical dosage forms and improves research and development work. Factorial designs, where all the factors involved are studied in all possible combinations, are considered to be the most efficient designs for estimating the influence of individual variables and their interactions using the minimum number of experiments. The use of factorial design in pharmaceutical formulation development has played a key role in gaining an understanding of the relationship between the independent variables and the responses obtained. All independent variables are controllable, and the responses are dependent upon the independent variables. The response surface plot gives a visual representation of the response. This helps the process of optimization by providing an empirical model equation for the response as a function of the different variables [9].

The objective of this investigation was to prepare, characterize, evaluate and optimize SLNs containing OND for CNS targeting in an animal model. We believe that the SLNs will enable rapid nose-to-brain transport of OND, thereby reducing the side effects, reducing the dose and

frequency of administration, reducing the cost of therapy and possibly improves patient compliance.

The optimized formulation obtained in this study was used in a gamma scintigraphic study conducted on rabbits. Gamma scintigraphy is a technique in which the transit of a dosage form to intended site can be non-invasively imaged in vivo via the judicious introduction of an appropriate short lived gamma emitting radioisotope [10].

2 Materials and methods

2.1 Materials

Glycerol monostearate (GMS) (Fine Chem Industries, Mumbai) was used as the lipid material for preparing SLNs. OND was kindly donated by West-Cost Pharmaceuticals Pvt. Ltd., Ahmedabad, India. Soya lecithin (surfactant) was received as a gift from PHOSPHOLIPID GmbH, Germany and Poloxamer 188 (cosurfactant) was bought from HiMedia Lab Pvt. Ltd, Mumbai, India. All other reagents used were of analytical grade. Double distilled water was used throughout the study.

2.2 Methods

2.2.1 Preparation of SLN

SLNs loaded with OND were prepared using the solvent diffusion method. The aqueous phase was prepared by dissolving the surfactant (Lecithin) and co-surfactant (Poloxamer 188) in 50 ml of double distilled water. The organic solution was prepared by completely dissolving the drug (OND) and lipid (GMS) in 5 ml of water-miscible solvent (ethanol) in a water bath at 70 °C, which is above the melting point of the GMS. The resultant organic solution was injected into 50 ml of an aqueous phase containing the surfactant, with mechanical stirring (Remi Instruments Ltd, Mumbai, India) at 1,000 rpm at 61 °C for 1 h. The nanosuspension formed was allowed to cool at room temperature. As the temperature drops under such conditions, the lipid droplets solidify producing SLNs [6]. Various variables such as the lipid, surfactant and co-surfactant concentrations were considered when optimizing the formulation (Table 1).

Table 1 Factorial design parameters and experimental conditions

Factors	Levels used, actual (coded)	
	Low (−1)	High (+1)
X_1 = lipid concentration (mg/ml)	10	15
X_2 = surfactant concentration (%)	0.5	1
X_3 = co-surfactant concentration (%)	0.5	1

2.2.2 Experimental design

Various batches of OND loaded SLNs were prepared on the basis of a 2^3 factorial design. The independent variables were lipid concentration (X_1), surfactant concentration (X_2) and concentration of co-surfactant (X_3). The independent variables and their levels are listed in Table 1. The particle size of the SLNs (Y_1) and the entrapment efficiency (Y_2) were treated as response parameters or dependent variables.

3 Evaluation of SLNs

3.1 Determination of particle size, polydispersity index, and zeta potential

Photon correlation spectroscopy (PCS, Zetasizer 3000, Malvern Instruments, UK) was used to measure the size and zeta potential (ZP) of the SLNs of all the drug-loaded samples. All samples were diluted with distilled water to make up a suitable concentration. The Z-average particle size, polydispersity index (PI), and zeta potential (ZP) were determined.

3.2 Total drug content (TDC)

The total amount of drug in the formulation was determined by dissolving 1 ml of the suspension in 10 ml of ethanol. The amount of OND in each sample was determined using a UV spectrophotometer (1700, Shimadzu, Japan) by measuring the absorbance at a λ_{max} value of 310 nm. Each experiment was performed in triplicate. A placebo formulation prepared using process similar to that used for preparing the samples was also subjected to spectrophotometric measurements. The total drug content was calculated using the following equation:

$$
\begin{aligned}
\text{TDC} = {} & \text{concentration} \times \text{dilution factor} \\
& \times \text{volume of formulation}
\end{aligned} \tag{1}
$$

3.3 Entrapment efficiency (EE)

The EE was determined by analyzing the free drug content in the supernatant obtained after centrifuging the SLN suspension in a high speed cooling centrifuge (Remi instruments Ltd, Mumbai, India) at 1,7000 rpm for 1 h at 0 °C. The EE was calculated as follows:

$$
\text{EE} = \frac{\text{total drug(Assay)} - \text{free drug}}{\text{total drug}} \times 100 \tag{2}
$$

3.4 In vitro drug release study

An in vitro drug release study of the SLNs ($n = 3$) was carried out using a Franz diffusion cell with a dialysis membrane (cut-off molecular weight 1,2000) in which the donor compartment contained a freeze dried sample and the receptor compartment was filled with a phosphate buffer solution (pH 6.6). The donor chamber was placed in such a way that it just touched the diffusion medium in the receptor chamber. The temperature was maintained at 37 ± 1 °C using a circulating water bath. Samples were periodically drawn from the receptor compartment and assayed using a UV spectrophotometer (1700, Shimadzu, Japan) at 310 nm [11]. When a sample was drawn, the same quantity of fresh prewarmed buffer solution was replaced.

3.5 Histological study

Sheep nasal mucosa was obtained from a local abattoir within 1 h of an animal being killed. The mucosa was cleaned by washing with an isotonic saline solution. Freeze dried SLNs were applied on the nasal mucosa. The nasal mucosa was then fixed in 10 % neutral carbonate buffered formalin solution and processed and embedded in paraffin according to standard procedures. The experiment was carried out in a cell culture incubator (MCO-5AC, Sanyo Incubator, Japan) to provide the optimal conditions for the viability of the tissues. Paraffin sections (7 μm) were cut on glass slides and stained with hematoxylin and eosin (HE). Sections were examined under a light microscope by a pathologist blinded to the study to detect any damage to the tissue during in vitro permeation [12].

3.6 Transmission electron microscopy (TEM)

Morphological examination of the optimized batch (F7) was carried out using a transmission electron microscope (CM200, Philips, Netherlands). Samples were stained with a solution of 2 % (w/v) osmium tetraoxide and finely spread over a slab for capturing images.

3.7 Differential scanning calorimetry

Differential scanning calorimetry (DSC) thermograms were recorded for OND, GMS and the freeze-dried OND loaded SLNs. Samples were placed on a DSC reference pan and thermograms were obtained using a differential scanning calorimeter (DSC 822c, Mettler Toledo, USA). The samples were heated from 0 °C to 300 °C under a nitrogen atmosphere at a heating rate of 10 °C/minute.

3.8 X-ray diffraction (XRD)

The crystallinity of the OND and freeze dried SLNs was evaluated by XRD using an X-ray diffractometer (D8 Advance, BruckerAxs, Germany). Samples were mounted on a sample holder and XRD patterns were recorded in the range from 3 to 80° at a chart speed of 5° per minute.

3.9 Stability study

All samples were freeze dried at −20 °C and maintained at this temperature for a period of 10 min. They were transferred to a lyophilizer (VirTis Benchtop, SP Industries, USA) and maintained under vacuum (30 mTorr) for a period of 6 h. The dried powder was then packed in glass vials. These vials, containing the optimized batch were sealed with rubber caps and maintained under ambient conditions of temperature and moisture (40 °C and 75 % RH) for a period of 3 months in a stability chamber (CHM-10S, Remi Lab, Mumbai, India). Every month, stability samples were re-dispersed in distilled water and the stability of the SLNs was evaluated by measuring the particle size and EE of the suspension.

3.10 Radiolabeling of OND SLN suspension

OND SLN suspension was radiolabeled with Technetium-99 m (^{99m}Tc) using the direct labeling method. Stannous chloride dihydrate (100 μg in 100 μL of 0.10 N HCl) was added to 0.6 ml of OND SLNs suspension. The pH was adjusted to 6.5 using a 50 mM sodium bicarbonate solution. Sterile ^{99m}Tc-pertechnetate was added with continuous mixing, and the mixture was incubated at 30 ± 5 °C for 30 min. The final volume was made up to 1.0 ml using a 0.9 % (w/v) sterile sodium chloride solution. The activity of the resultant solution was 5 mCi/ml.

The radiochemical purity of the ^{99m}Tc-labeled OND SLNs was determined using ascending instant thin layer chromatography (TLC) with silica gel-coated fiberglass sheets (Gelman Sciences Inc, Ann Arbor, MI). Acetone was used as the mobile phase. The effects of incubation time, pH and stannous chloride concentration on labeling were studied to obtain the optimum reaction conditions. The optimized, stable radiolabeled-drug formulation was used to study CNS targeting in rabbits [13–15].

3.11 Gamma scintigraphic imaging

In vivo studies were performed in accordance with the guidelines approved by the Committee for the Purpose of Control and Supervision of Experiments on Animals, Ministry of Social Justice and Empowerment, Government of India. The study protocol was duly approved by the Institutional Animal Ethics Committee of R. C. Patel Institute of Pharmaceutical Education & Research, Shirpur, India (Reg. No. 651/02/C/CPCSEA).

New Zealand white rabbits (2.00–2.50 kg) were selected for the study. The radiolabeled complex of ^{99m}Tc-OND SLNs (5 mCi/ml) was administered (0.5 ml) in each nostril. The backs of the rabbits were held such that they slanted backwards during nasal administration of the formulations. All the animals were conscious throughout the experiments and were held in rabbit restrainers during the scintigraphic study. Imaging was performed by single photon emission computerized tomography (SPECT, LC 75-005, Diacam, Siemens AG, Erlanger, Germany).

3.12 Optimization data analysis and model-validation

ANOVA was used to establish the statistical validation of polynomial equations generated by Design Expert® software (version 8.0.1.0, Stat-Ease Inc., Minneapolis, MN, USA). Fitting a multiple linear regression model to a 2^3 factorial design gave a predictor equation which was a first-order polynomial, having the form:

$$Y = b_0 + b_1X_1 + b_2X_2 + b_3X_3 + b_{12}X_1X_2 + b_{13}X_1X_3 + b_{23}X_2X_3 + b_{123}X_1X_2X_3 \tag{3}$$

where, Y is the measured response associated with each factor level combination; b_0 is an intercept representing the arithmetic average of all quantitative outcomes of eight runs; b_1–b_{123} are regression coefficients computed from the observed experimental values of Y; and X_1, X_2 and X_3 are the coded levels of the independent variables. The terms X_1X_2, X_2X_3 and X_1X_3 represent the interaction terms. The main effects (X_1, X_2 and X_3) represent the average result of changing one factor at a time from its low value to its high value. The interaction terms show how the response changes when two factors are changed simultaneously. The polynomial equation was used to draw conclusions based on the magnitude of the coefficients and the mathematical sign it carries, i.e. positive or negative. A positive sign signifies a synergistic effect, whereas a negative sign stands for an antagonistic effect.

In the model analysis, the responses (the particle size of SLNs and the EE) of all model formulations were processed using Design Expert® software. The best fitting mathematical model was selected based on the comparisons of several statistical parameters including the coefficient of variation (CV), the multiple correlation coefficient (R^2), the adjusted multiple correlation coefficient (adjusted R^2) and the predicted residual sum of square (PRESS), provided by Design Expert® software. The level of significance was considered at $P < 0.05$. Three-dimensional response surface plots and two-dimensional contour plots were created using Design Expert®. Subsequently, the desirability approach was used to generate the optimum settings for the formulations [9].

Linear model: $$Y = b_1X_1 + b_2X_2 + b_3X_3 \tag{4}$$

2FI (interaction) model: $$Y = b_1X_1 + b_2X_2 + b_3X_3 + b_{12}X_1X_2 + b_{13}X_1X_3 + b_{23}X_2X_3 \tag{5}$$

4 Results and discussion

4.1 Preparation of SLNs dispersion

When the solvent diffusion method is used with an aqueous system, the diffusion rate of the water miscible organic solvent into the aqueous phase is very rapid. Turbulence occurs at the interface of the emulsion droplets because of the Marangoni effect. The surfactant and co-surfactant in the aqueous phase are adsorbed around the emulsion droplets, resulting in the spontaneous formation of droplets, the size of which is in the submicron range [16].

5 Evaluation of SLNs

5.1 Particle size, polydispersity index and zeta potential

The particle size, polydispersity index (PDI) and zeta potential (ZP) values of the SLNs prepared were found to be in the ranges from 320 to 498 nm, 0.296 to 0.446 and −10.9 to −16.5 mV, respectively (Table 2). The particle size was found to be significantly affected with an increase in the amount of lipid at a lower surfactant concentration. As the GMS concentration increases from 50 to 75 mg the mean particle size of the formulation increases (Table 2). This may be attributed to the inability of the surfactant solution to stabilize the emulsion at a very low concentration (0.5 %). A higher concentration of surfactant was sufficient to stabilize the emulsion even with a high lipid load of 75 mg, with a consistent particle size.

It was observed that varying the concentrations of lecithin affected the SLNs particle size significantly. The particle size was found to decrease with increasing lecithin concentration with the amount of lipid remaining constant (Table 2). We attribute this effect mainly to the increasing viscosity of the lecithin solution. During the process of emulsification, the droplet size decreases under the influence of the high shear. At the same time, the droplets have a tendency to form aggregates so that the surface energy is reduced. However, the presence of surfactant molecules stabilizes the emulsion by forming a thick protective layer around the droplets which prevents them from coalescing.

The combination of surfactant and cosurfactant displayed a synergistic effect and thus reduced the particle size and prevented particle agglomeration more efficiently. Therefore, lecithin and poloxamer 188 were selected for formulation of SLNs. Lecithin stabilizes the suspension by electrostatic repulsion since it is an amphoteric surfactant, whereas poloxamer 188, a non ionic surfactant, stabilizes the suspension sterically [17]. As more poloxamer 188 is added the particle size decreases, stabilizing the dispersion of SLNs (Table 2). It has been reported that SLNs stabilized with surfactant mixtures have lower particle size and higher storage stability compared with formulations with only one surfactant [18].

The measurement of the zeta potential (ZP) allows prediction about the stability of colloidal dispersion. The ZP is the electric charge on the surface of particle which creates an electrical barrier, and acts as a 'repulsive factor' in the process of stabilization of an emulsion. A high surface energy plays a major role in improving the stability of the formulation as like charges at the interface resists coalescence of particles [19]. The ZP of the SLNs was found to possess a negative surface charge due to the presence of negatively charged GMS. The change in the ZP was not found to vary significantly (−10.9 to −16.5 mV) with a change in either of the operating variables as shown in Table 2. Optimized batch F7 was found to have sufficient stability despite its very low ZP value (−16.5 mV). This indicates that a factor other than ZP is responsible for the stability of the formulation which may be the presence

Table 2 Formulation of the SLN utilizing a 2^3 factorial design

Batch code	X_1	X_2	X_3	Y_1	Y_2	Zeta potential (mV)	PDI
F1	10	0.5	0.5	398.1	32.89	−12.2	0.389
F2	15	0.5	0.5	498.1	41.42	−10.9	0.372
F3	10	1	0.5	344.8	37.56	−11.5	0.385
F4	15	1	0.5	433.9	44.12	−11.8	0.409
F5	10	0.5	1	352	39.09	−14	0.446
F6	15	0.5	1	442.4	46.88	−15	0.346
F7	10	1	1	320	49.69	−16.5	0.296
F8	15	1	1	360	56.56	−14	0.349

Y_1 and Y_2 are particle size (nm) and entrapment efficiency (%) respectively

X_1 lipid concentration, X_2 surfactant concentration, X_3 co-surfactant concentration

of a steric stabilizer (Poloxamer 188) that can easily compensate for the missing electrostatic repulsion and stabilize the dispersion for a longer time [20].

5.2 Entrapment efficiency

The effect of the independent variables on the EE of the SLNs was significantly affected, unlike the particle size, at every level of study. An increase in EE was observed with increasing surfactant and co-surfactant concentration (Table 2). This is believed to occur as the surfactant reduces the interfacial tension between the lipid and aqueous phase. As expected, the EE was found to be increased with increasing amount of lipid (Table 2), which may be due to a greater availability of lipid to encapsulate the drug.

5.3 In vitro drug release

The dissolution profile indicates biphasic behavior consisting of an initial burst release, followed by a phase of slow release (Fig. 1). The initial burst release may be attributed to the presence of free drug in the external phase and drug adsorbed onto the surface of particles, while the slow release may be due to the drug encapsulated within the lipid matrix. In order to understand the mechanism and kinetics of drug release, the data were analyzed using the Peppas equation, $M_t/M_\infty = kt^n$, where M_t is the amount of drug released at time t, M_∞ is the amount released at time ∞, M_t/M_∞ is the fraction of drug released at time t, k is a constant for characteristic of the drug-polymer system and n is the diffusion exponent, a measure of the primary mechanism of drug release. The values of n and the correlation coefficient (r) were estimated using the least squares procedure. In spherical matrices, if $n \leq 0.5$, a Fickian diffusion (case-I) dominates; $0.45 \leq n < 0.9$, anomalous or non-Fickian transport dominates; and $n \geq 0.9$, a case-II transport (zero order) drug release mechanism dominates. The value of n was found to be
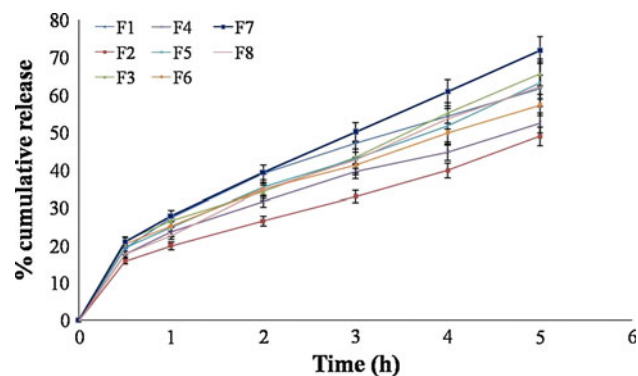
0.483 for optimized batch, with the correlation coefficient being 0.990, indicating a Fickian type of transport. The release kinetics followed the Higuchi model. This shows that the release of drug from the optimized SLNs formulation may be attributed primarily to the diffusion of the drug from the pores on the surface of the particles.

5.4 Histological study

It is necessary to examine the histological changes caused by formulations in the nasal mucosa if they are to be considered for practical use. Control mucosa (untreated nasal mucosa) stained with hematoxylin–eosin (Fig. 2(A_1)) and sheep nasal mucosa on which the formulations were applied (Fig. 2(A_2)) were studied histologically. No change in mucosal structure was observed when compared control and treated mucosa.

5.5 Transmission electron microscopy (TEM)

The shape and surface morphology of SLNs of optimized batch F7 was studied using TEM. The TEM micrograph obtained revealed that the solvent diffusion process lead to the formation of spherical nanoparticles with smooth surface and uniform size distribution (Fig. 2b).

5.6 Differential scanning calorimetry (DSC)

DSC is a very useful technique for detecting drug-excipient interactions in formulations. OND, GMS and SLNs formulation was studied using DSC. For the bulk material of GMS, the melting process took place with maximum peak at 58.05 °C. DSC thermogram of freeze dried SLN showed an endotherm at 54.73 °C, which can be attributed to melting of GMS in SLN (Fig. 3). The transformation of a sharp to a broad DSC peak is associated with the formation of amorphous regions in which the drug was molecularly dispersed [21].

5.7 X-ray diffraction (XRD)

XRD spectra's of pure (OND), bulk GMS and freeze dried SLNs are presented in Fig. 4. The XRD pattern of OND shows a principal peak of 2θ between 5 and 25°. The GMS pattern has a principal peak of 2θ at around 19.30°. The principal peak of OND was absent in OND-loaded SLN formulations; furthermore, the principal peak of the lipid did not shift but was less pronounced. This may be attributed to the incorporation of OND between parts of the crystal lattice of the lipid, leading to a change in the crystallinity of the OND- loaded SLNs from a crystalline form to an amorphous form.
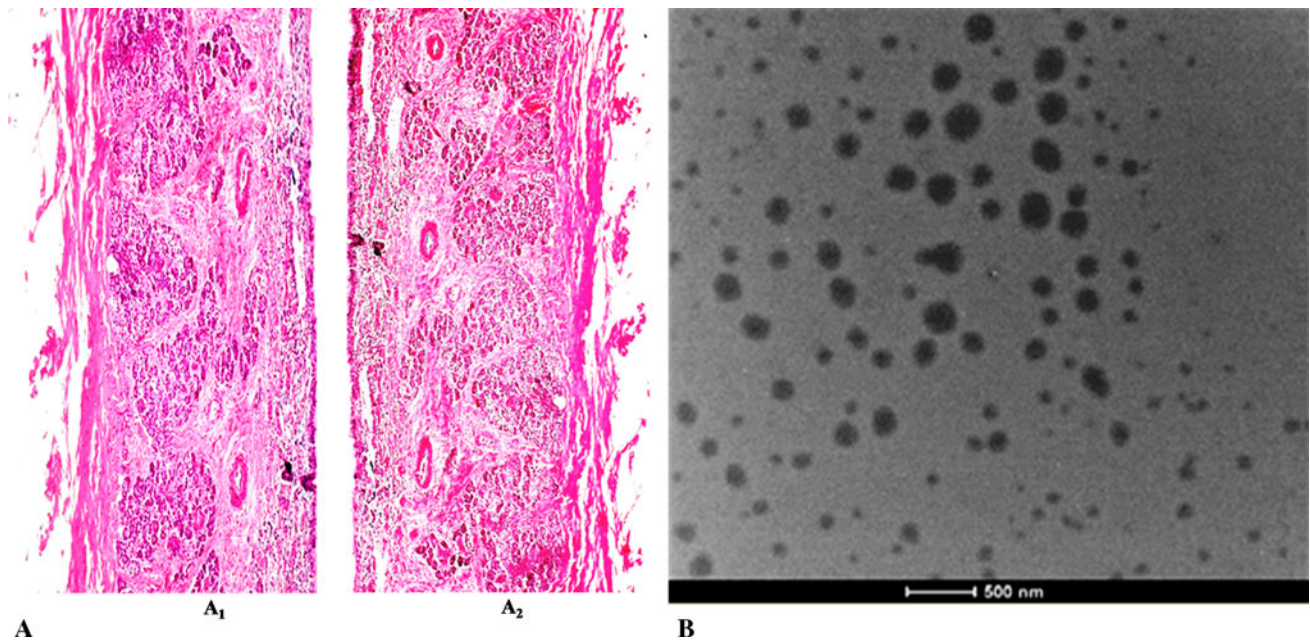

Fig. 1 In vitro drug release of ondansetron HCl from SLN

Fig. 2 **a** Light photomicrograph of the nasal mucosa (A_1) untreated nasal mucosa (A_2) SLN treated nasal mucosa. **b** TEM image of optimized formulation
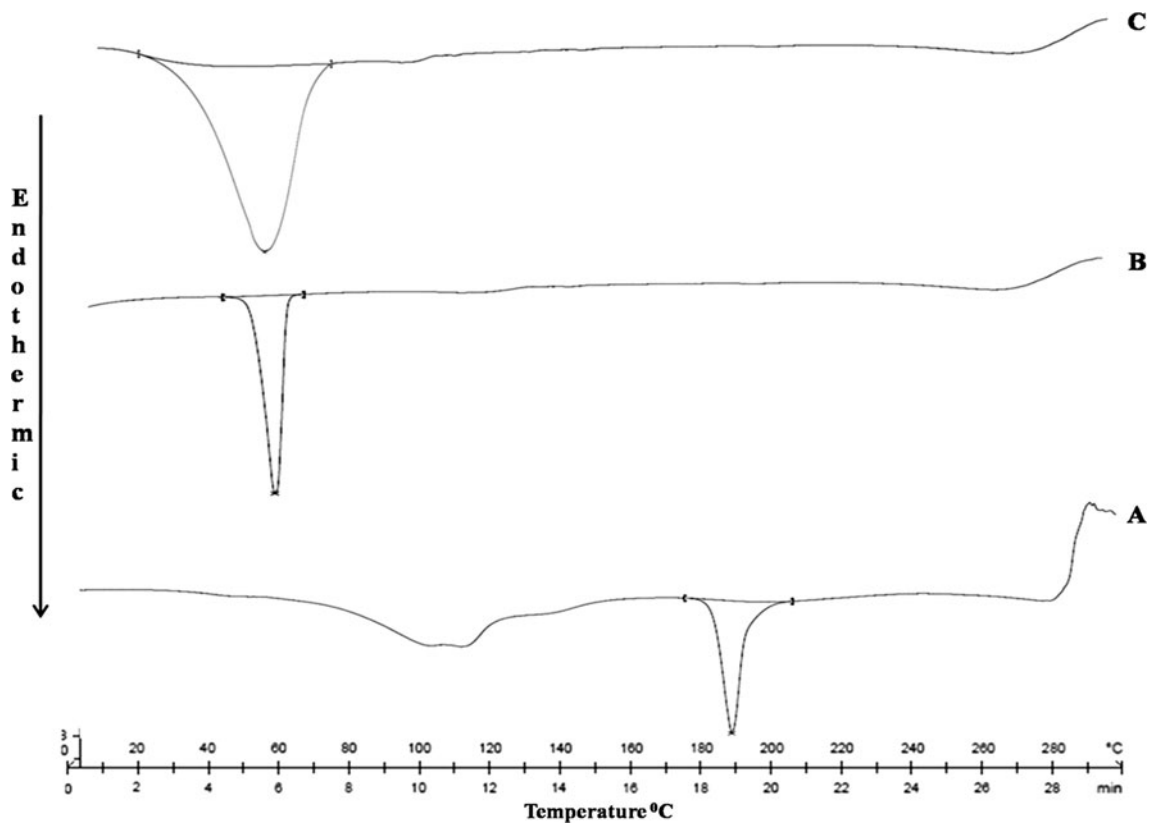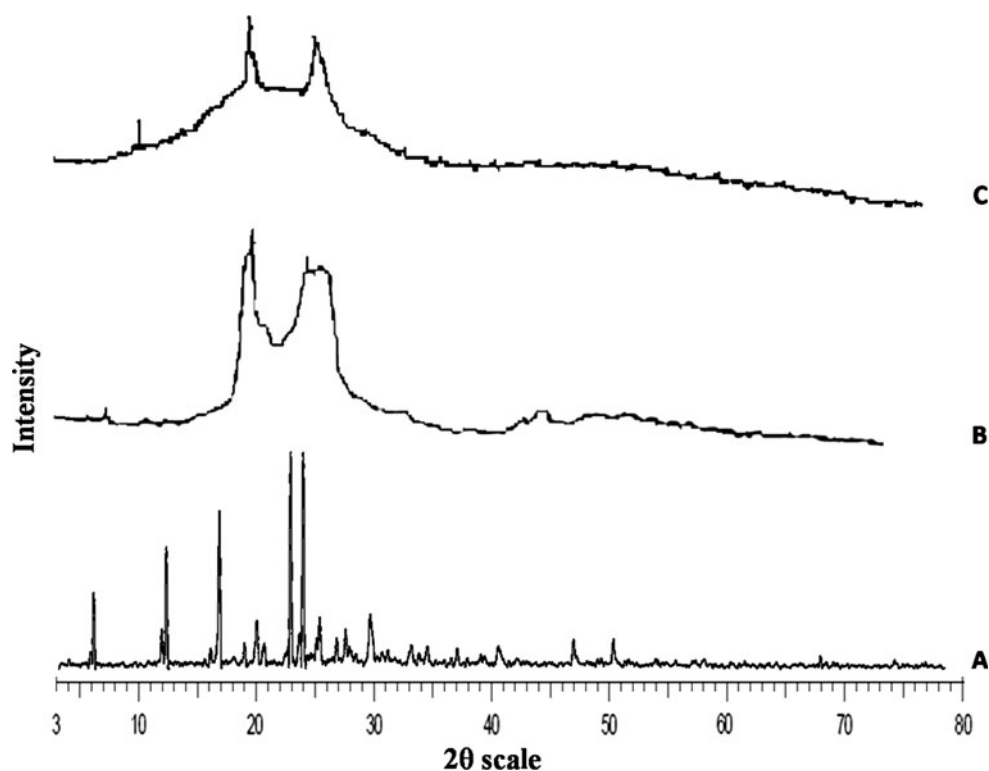

Fig. 3 DSC thermogram of **a** OND, **b** GMS and **c** OND loaded SLN

Fig. 4 X-ray diffractogram of **a** OND, **b** GMS and **c** OND loaded SLN

5.8 Stability study

The effect of temperature and humidity on particle size and EE during storage is shown in Table 3. It was found that the formulation was stable for 3 months. The particle size increased only slightly, from 320 to 364.4 nm, during the stability study. This indicates that the system is stable for 3 months under accelerated testing conditions. The EE after 3 months of the optimized batch (42.1 %) indicated that the drug was retained within the nanoparticles throughout the stability study.

5.9 Radiolabeling of OND SLN suspension

The formulation was effectively radiolabeled with technetium-99 m (^{99m}Tc), which was optimized for maximum labeling efficiency and stability. When the formulation was evaluated for reduced/hydrolyzed (R/H) ^{99m}Tc and free ^{99m}Tc, the radiochemical purity achieved was determined to be 97.03 %. The optimal $SnCl_2 \cdot 2H_2O$ concentration was

found to be 100 μg/ml at a pH value of 6.5, with an incubation time of 30 min.

5.10 Gamma scintigraphic imaging

Scintigraphic images obtained from rabbits at 1, 2, 4 and 6 h after i.n. administration are shown in Fig. 5. They clearly demonstrates a rapid accumulation of radio-labeled drug in the brain following i.n. administration, followed by distribution to various organs. The literature reveals that the drug uptake into the brain from the nasal mucosa mainly occurs via the olfactory pathway by which the drug partly travels from the nasal cavity to the CSF and/or brain tissue [13]. It can be concluded that the drug in the brain tissue after i.n. administration has passed mainly through this pathway. However, SLNs which are smaller than 100 nm in size may pass through the BBB, increasing the level of drug-loaded SLNs in the brain.

Figure 5 showed that the formulation was cleared slowly and was retained for an extended period in the brain, thereby providing rapid and enhanced action.

5.11 Optimization data analysis and model-validation

5.11.1 Fitting of data to the model

Three factors with lower and upper design points in coded and uncoded values are listed in Table 1. The ranges of

Table 3 E.E. and particle size during stability study

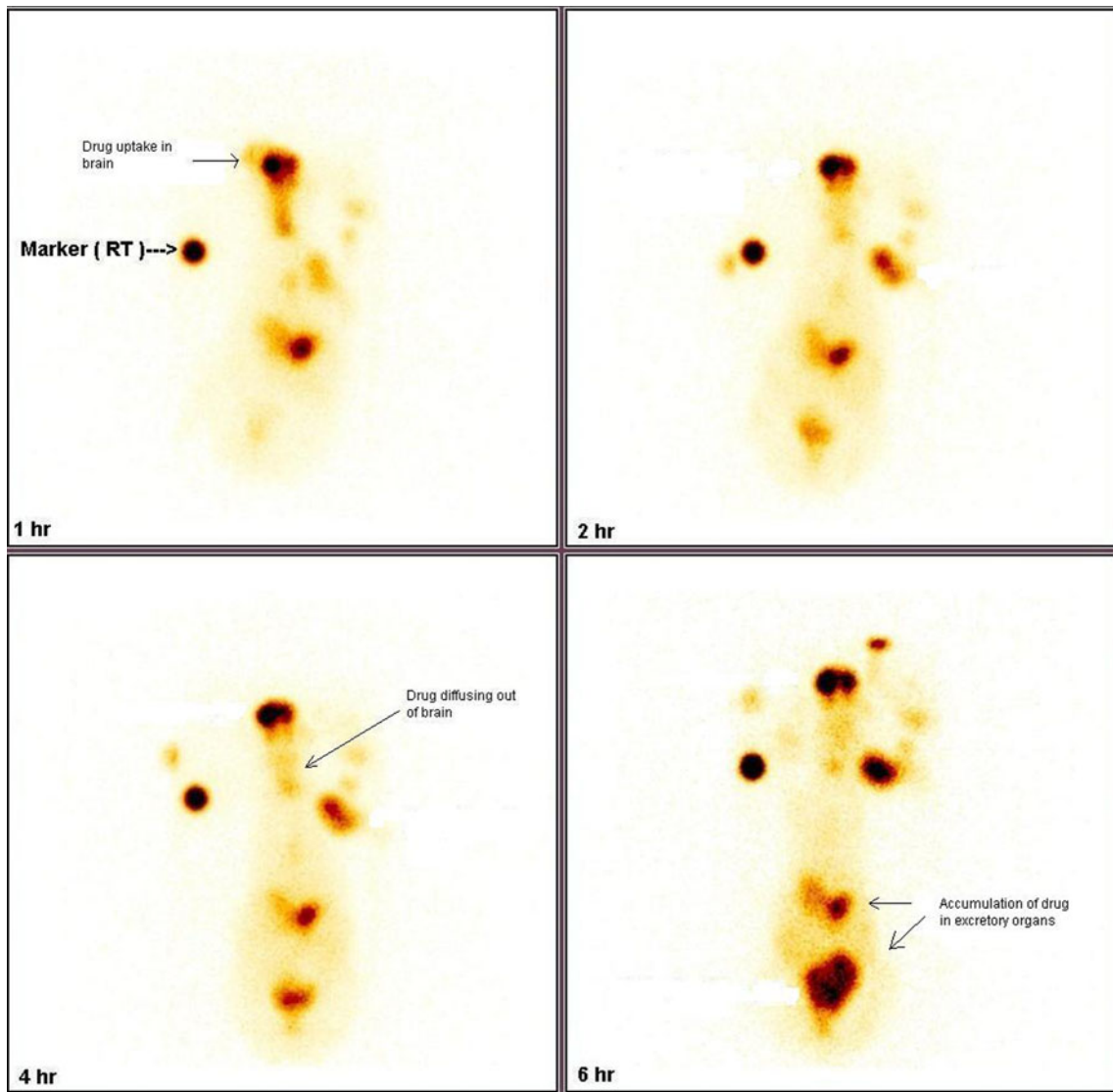| Time in days	E.E.	Particle size
30	48.31	328.2
60	45.44	346.8
90	42.1	364.4

Fig. 5 Scintigraphy image of rabbit following intranasal administration of SLN to nasal cavity

Table 4 Summary of results of regression analysis for responses Y_1 and Y_2

Models	R^2	Adjusted R^2	Predicted R^2	SD	%CV
Response (Y_1)					
Linear model	0.9572	0.9250	0.8287	16.56	4.21
Response (Y_2)					
2F1 model	0.9996	0.9975	0.9775	0.37	0.85

Regression equations of the fitted linear and interactive model: $Y_1 = 393.66 + 39.94X_1 - 28.99X_2 - 25.06X_3$; $Y_2 = 43.53 + 3.72X_1 + 3.46X_2 + 4.53X_3 - 0.36X_1X_2 - 0.054X_1X_3 + 1.61X_2X_3$

responses Y_1 and Y_2 were found to be 320–498.1 nm and 32.89–56.56 %, respectively. All the responses observed for eight formulations were fitted to various models using Design-Expert®. It was observed that the best-fitted

models were linear for both particle size and EE. But the 2FI model was selected for EE because it showed an interactive effect on the responses of the independent variables, unlike the linear model. The R^2, adjusted R^2,

Table 5 Results of analysis of variance for measured response

Parameters	DF	SS	MS	F	Significance F
Particle size					
Model	3	24507.26	8169.09	29.80	0.0034 significant
Residual	4	1096.66	274.16	–	–
Total	7	25603.92	8443.25	–	–
E.E.					
Model	6	392.18	65.36	474.29	0.0351 significant
Residual	1	0.14	0.14	–	–
Total	7	392.32	65.5	–	–

DF degrees of freedom, *SS* sum of square, *MS* mean sum of square, *F* Fischer's ratio
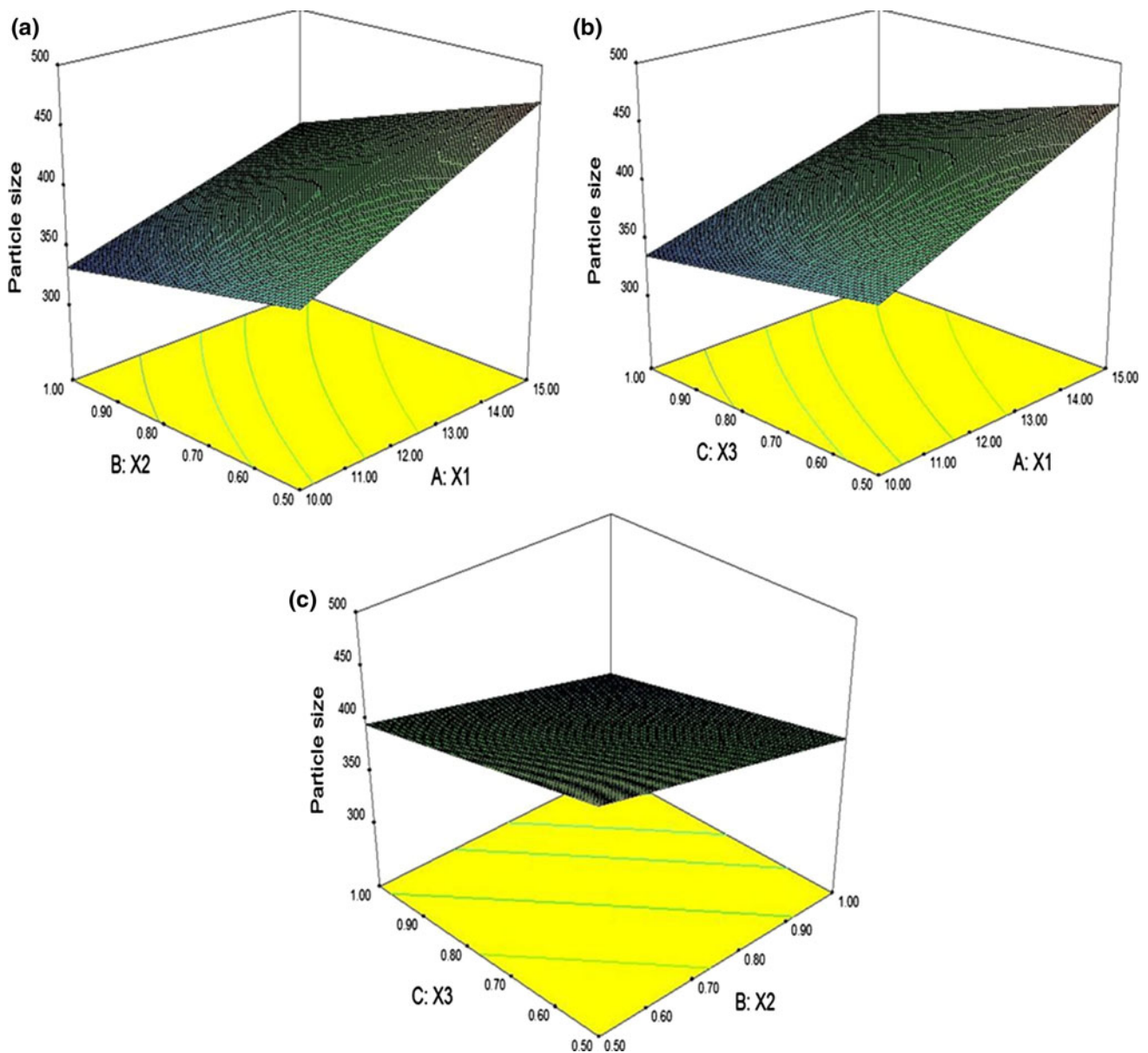
Fig. 6 Response surface plots for the **a** X_1 and X_2, **b** X_1 and X_3 and **c** X_2 and X_3 on particle size (Y_1), where, X_1 = lipid concentration, X_2 = surfactant concentration, X_3 = co-surfactant concentration

predicted R^2, SD and %CV values are given in Table 4, along with the regression equation generated for each response. The ANOVA results in Table 5 for the dependent variables demonstrate that the model was significant for both response variables.

It was observed that the independent variables X_2 (surfactant concentration) and X_3 (concentration of co-surfactant) had a negative effect, while, X_1 (lipid concentration) had a positive effect on particle size (Y_1). It was observed that all the three independent variables viz. X_1, X_2 and X_3, had a positive effect for EE.

The coefficients with more than one factor term in the regression equation represent interaction terms. It also suggests that the relationship between factors and responses is not always linear. When more than one factor is changed simultaneously and used at different levels in a formulation, a factor can produce different degrees of response. The interaction effects of X_1 and X_2; and of X_1 and X_3 were unfavorable (negative), whereas the interaction effect of X_2 and X_3 was favorable (positive) for response Y_2.

5.11.2 Response surface analysis

Three dimensional response surface plots generated using Design Expert® are presented in Figs. 6 and 7. They show the responses of the particle size and EE. Fig. 6a shows the response surface plots of lipid (X_1) and surfactant (X_2) concentration against particle size. X_1 increases linearly when X_2 increases and the particle size was found to
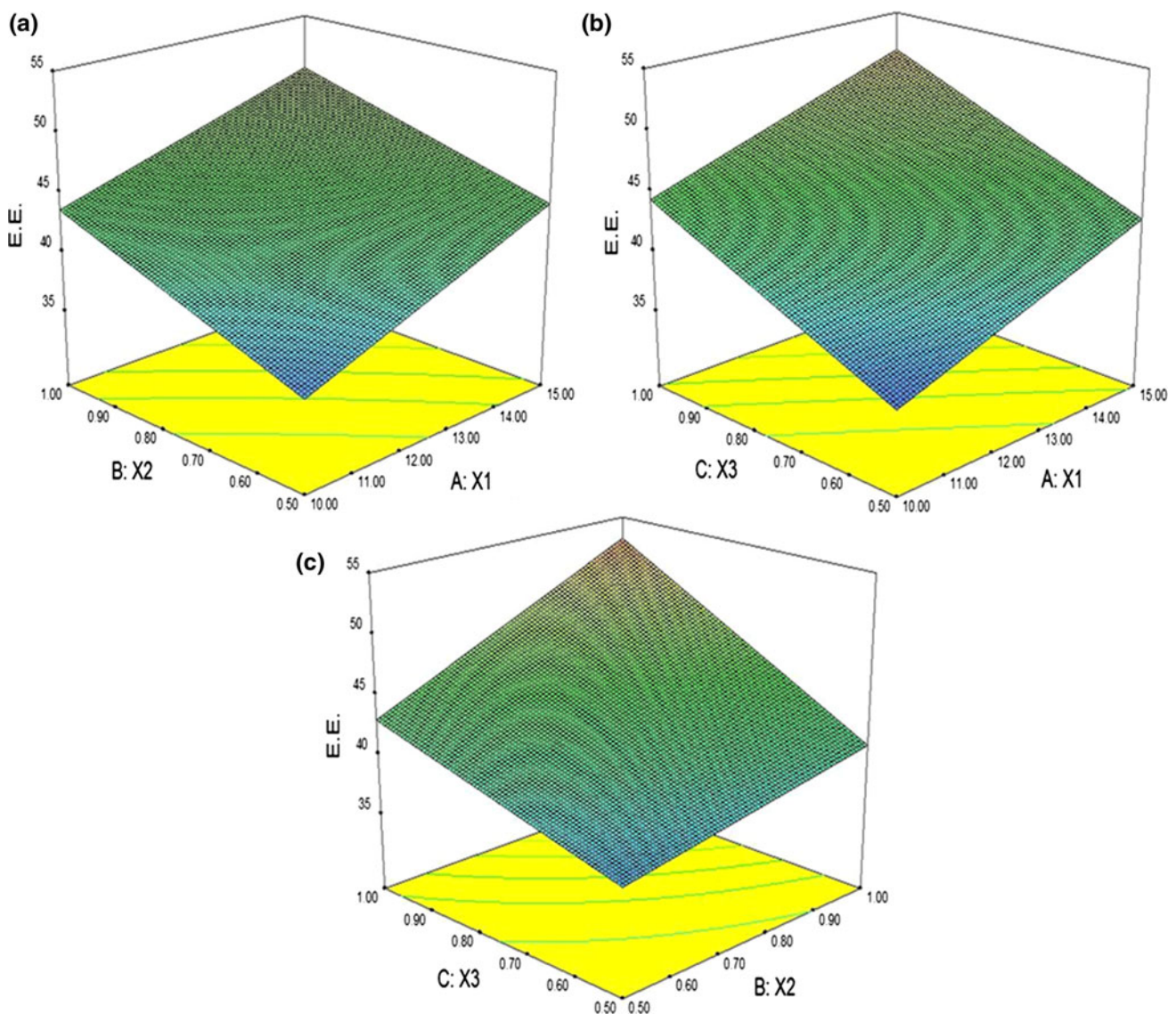

Fig. 7 Response surface plots for the **a** X_1 and X_2, **b** X_1 and X_3 and **c** X_2 and X_3 on E.E. (Y_2), where, X_1 = lipid concentration, X_2 = surfactant concentration, X_3 = co-surfactant concentration

decrease. Similar effects were observed for factors X_1 and X_3 (Fig. 6b). The combined effect of X_2 and X_3 on particle size of SLNs was observed to be non-linear, as shown in Fig. 6c. At higher surfactant and co-surfactant concentration, a lower particle size was observed. Figure 7 shows the response surface plots of the effect of X_1 (lipid concentration) and X_2 (surfactant concentration) on EE. A linear effect is indicated. The combined effects of X_2 and X_3 and of X_1 and X_3 were also linear. This indicates that with greater amount of lipid, the EE will be higher.

5.11.3 Optimization and validation

A numerical optimization technique by the desirability approach was used to generate the optimum settings for the formulation. The process was optimized for the dependent variables Y_1 and Y_2. The formulation was optimized such that it would have smallest particle size, with sufficient EE. Formulation F7, with 10 mg/ml lipid, 1 % surfactant and 1 % co-surfactant fulfilled all the criteria.

Table 6 provides comparison of the observed and predicted values of responses Y_1 and Y_2 for all the formulations. It can be seen that in all cases there was a reasonable agreement between the predicted and experimental values. It can thus be concluded that the equations describe adequately the influence of the selected independent variables on the responses studied. This indicates that the optimization technique was appropriate for optimizing the OND

Table 6 The predicted and observed response variables of the OND loaded SLN

Responses	Formulation	Predicted value	Observed value	Prediction error (%)
Y_1	F1	398.1	407.77	2.42
	F2	498.1	487.65	−2.09
	F3	344.8	349.8	1.45
	F4	433.9	429.67	−0.97
	F5	352	357.65	1.60
	F6	442.4	437.52	−1.10
	F7	320	299.67	−6.35
	F8	360	379.55	5.43
Y_2	F1	32.89	33.02	0.39
	F2	41.42	41.28	−0.33
	F3	37.56	37.42	−0.37
	F4	44.12	44.25	0.29
	F5	39.09	38.95	−0.35
	F6	46.88	47.01	0.27
	F7	49.69	49.82	0.26
	F8	56.56	56.42	−0.24

Prediction error (%) = (Observed value − Predicted value)/Predicted value × 100 %

Y_1 and Y_2 are particle size and in E.E., respectively

loaded SLN formulation. The low magnitudes of error found in the present investigation demonstrate the high prognostic ability of the technique of optimization using factorial design.

6 Conclusion

A significant quantity of OND was rapidly delivered to the brain by i.n. administration of the SLNs that were formulated. The radio-imaging study conducted on rabbits clearly demonstrated the effectiveness of i.n. delivery of OND in the form of SLNs. In conclusion, the results of the present study indicate that delivering OND intranasally for targeting the CNS to achieve immediate onset of action has considerable potential.

References

1. Gasco MR. Lipid nanoparticles: perspectives and challenges. Adv Drug Deliv Rev. 2007;59:377–8.
2. Mehnert W, Mader K. Solid lipid nanoparticles: production, characterization, and applications. Adv Drug Deliv Rev. 2001;47:165–96.
3. Hu FQ, Hong Y, Yuan H. Preparation and characterization of solid lipid nanoparticles containing peptide. Int J Pharm. 2004;273:29–35.
4. Zhang N, Ping Q, Huang G, Xu W, Cheng Y, Han X. Lectin-modified solid lipid nanoparticles as carriers for oral administration of insulin. Int J Pharm. 2006;327:153–9.
5. Varshosaz J, Ghaffari S, Khoshayand MR, Atyabi F, Azarmi S, Kobarfard F. Development and optimization of solid lipid nanoparticles of amikacin by central composite design. J Liposome Res. 2010;20(2):97–104.
6. Zhang J, Fan Y, Smith E. Experimental design for the optimization of lipid nanoparticles. J Pharm Sci. 2009;98:1813–9.
7. Trotta M, Debernardi F, Caputo O. Preparation of solid lipid nanoparticles by a solvent emulsification–diffusion technique. Int J Pharm. 2003;257:153–60.
8. Mahajan HS, Gattani SG. Nasal administration of ondansetron using a novel microspheres delivery system. Pharm Dev Tech. 2009;14(2):226–32.
9. Patil SB, Sawant KK. Development optimization and in vitro evaluation of alginate mucoadhesive microspheres of carvedilol for nasal delivery. J Microencapsul. 2009;26(5):432–43.
10. Digenis GA, Sandefer EP, Page RC, Doll WJ. Gamma scintigraphy: an evolving technology in pharmaceutical formulation development—part 1. PSTT. 1998;3:100–8.
11. Kaur IP, Bhandari R, Bhandari S, Kakkar V. Potential of solid lipid nanoparticles in brain targeting. J Control Release. 2008;127:97–109.

12. Jain SA, Chauk DS, Mahajan HS, Tekade AR, Gattani SG. Formulation and evaluation of nasal mucoadhesive microspheres of Sumatriptan succinate. J Microencapsul. 2009;29(8):711–21.

13. Kumar M, Misra A, Babbar AK, Mishra AK, Mishra P, Pathak K. Intranasal nanoemulsion based brain targeting drug delivery system of risperidone. Int J Pharm. 2008;358:285–91.

14. Vyas TK, Babbar AK, Sharma RK, Singh S, Misra A. Intranasal mucoadhesive microemulsions of clonazepam: preliminary studies on brain targeting. J Pharm Sci. 2006;95(3):570–80.

15. Saha GB. Methods of radiolabeling. In: Saha GB, editor. Physics and radiobiology of nuclear medicine. New York: Springer.

16. Hu FQ, Yuan H, Zhang HH, Fang M. Preparation of solid lipid nanoparticles with clobetasol propionate by a novel solvent diffusion method in aqueous system and physicochemical characterization. Int J Pharm. 2002;239:121–8.

17. Muller RH, Jacobs C. Buparvaquone mucoadhesive nanosuspension: preparation, optimization and long term stability. Int J Pharm. 2002;237:151–61.

18. Siekmann B, Westesen K. Melt-homogenized solid lipid nanoparticles stabilized by the nonionic surfactant tyloxapol I. Preparation and particle size determination. Pharm Pharmacol Lett. 1994;3:194–7.

19. Singh S, Dobhal AK, Jain A, Pandit JK, Chakraborty S. Formulation and evaluation of solid lipid nanoparticles of a water soluble drug: zidovudine. Chem Pharm Bull. 2010;58(5):650–5.

20. Schwarz C, Mehnert W, Lucks JS, Muller RH. Solid lipid nanoparticles (SLN) for controlled drug delivery. I. Production, characterization and sterilization. J Control Rel 1994;30: 83–96.

21. Singh KK, Pople PV. Development and evaluation of topical formulation containing solid lipid nanoparticles of vitamin A. AAPS PharmSciTech. 2006;7(4):E63–9.